k_2 is attributable to a reduction of the barrier in protonation caused by an increase in the excited-state basicity.

Acknowledgment. This work was supported by the Joint Studies Program (1985–1986) of the Institute for Molecular Science. H.K. thanks Professor R. Watts, University of California, Santa Barbara, CA, for helpful comments.

Supplementary Material Available: Derivation of eq 3–5 (2 pages). Ordering information is given on any current masthead page.

Contribution from the Department of Chemistry, The University of Calgary, Calgary, Alberta T2N 1N4, Canada, and Laboratory of Solid State Chemistry and Mössbauer Spectroscopy and Laboratories for Inorganic Materials, Department of Chemistry, Concordia University, Montreal, Quebec H3G 1M8, Canada

Lewis Base Properties of 1,5-Diphosphadithiatetrazocines: Crystal and Molecular Structures of 1,5-$Ph_4P_2N_4S_2Me^+CF_3SO_3^-$

Tristram Chivers,*[†] Georges Y. Dénès,[‡] Stephen W. Liblong,[†] and John F. Richardson[†]

Received March 21, 1989

The behavior of 1,5-$Ph_4P_2N_4S_2$ (**2**; R = Ph) toward Lewis and Brønsted acids has been investigated, and the following adducts have been isolated: 1,5-$Ph_4P_2N_4S_2H^+BF_4^-$, 1,5-$Ph_4P_2N_4S_2Me^+CF_3SO_3^-$, 1,5-$Ph_4P_2N_4S_2\cdot BCl_3$, [1,5-$Ph_4P_2N_4S_2H_2^{2+}$][$CF_3SO_3^-$]$_2$ and (1,5-$Ph_4P_2N_4S_2)_4\cdot 3SnCl_4$. The monoadducts show two equally intense doublets ($^4J_{PP}$ = 16–23 Hz) in the ^{31}P NMR spectra and exhibit a strong Raman band at 280–290 cm^{-1} attributed to an S–S stretching vibration. The structure of 1,5-$Ph_4P_2N_4S_2Me^+CF_3SO_3^-$ (**3**) has been determined by X-ray crystallography. The crystals of **3** are monoclinic, space group $P2_1/n$, with a = 14.231 (6) Å, b = 10.824 (3) Å, c = 19.326 (10) Å, β = 100.11 (4)°, V = 2930 (1) Å^3, Z = 4. The final R and R_w values were 0.075 and 0.078, respectively. The folded conformation of the $P_2N_4S_2$ ring is retained in **3**, and the cross-ring S–S interaction of 2.44 Å is significantly shorter than that of **2** (R = Ph) (d(S–S) = 2.53 Å). Coordination also causes a lengthening of the P–N and, especially, the S–N bonds involving the coordinated nitrogen to 1.67 and 1.68 Å from 1.62 and 1.60 Å, respectively, in **2** (R = Ph). The sum of the angles at the coordinated nitrogen atom is 358.0°. The ^{119}Sn Mössbauer spectrum of (1,5-$Ph_4P_2N_4S_2)_4\cdot 3SnCl_4$ consists of a single line with δ = 0.73 mm s^{-1}, and the ^{31}P NMR spectrum of a solution of this complex shows a singlet at 111.6 ppm. A weakly coordinated structure involving three hexacoordinated tin atoms with trans-bridging 1,5-$Ph_4P_2N_4S_2$ ligands is proposed to account for these data. The ^{31}P NMR spectra of the diadducts 1,5-$Ph_4P_2N_4R_2^{2+}$ (R = H, Me) indicate the presence of symmetrically and asymmetrically substituted isomers that interconvert in solution.

Introduction

Recently we reported the interaction of the 1,3-diphosphadithiatetrazocine **1** (R = Ph) with Lewis and Brønsted acids.[1] It was observed that monoadduct formation occurs at a nitrogen between phosphorus and sulfur and, on the basis of an X-ray structural determinations of the methylated derivative, results in lengthening of the bonds (particularly from sulfur) to the coordinated nitrogen. The resulting polarization of π-electron density in the ring produces an $-N{=}S{=}N-$ unit in the planar S_2N_3 moiety, which forms an angle of 108° with the PNP plane. The formation of symmetrical diadducts was also inferred on the basis of ^{31}P NMR data.

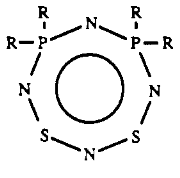

1

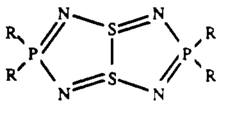

2

1,5-Diphosphadithiatetrazocines (**2**; R = Me, Ph), which are structural isomers of **1**, have been isolated and shown by X-ray crystallography to have folded structures with a weak cross-ring S–S interaction.[2,3] The low yields of the early syntheses of **2**, however, limited investigations of their reactivity to the oxidative addition of halogens, which occurs at the sulfur centers to give a trans-dihalogenated ring with loss of the S–S bond.[4] Recent improvements in the preparation of **2** (R = Me, Ph)[5] have facilitated further studies, and we describe here the Lewis base properties of **2** (R = Ph). No ambiguity exists over the site of coordination for monoadducts of **2**, since all four nitrogen atoms are chemically equivalent. However, the effect of adduct formation on ring conformation, particularly with regard to the loss or retention of the cross-ring S–S interaction, is of interest. The possible formation of diadducts, for which there are three structural isomers, is also worthy of attention.

The ring system **2** can be viewed as a hybrid of cyclotetraphosphazenes, $(R_2PN)_4$, and S_4N_4. For comparison, we note that the formation of monoprotonated derivatives of $(Me_2PN)_4$ gives rise to a minor perturbation of the ring conformation and an alternation of P–N bond lengths, the longest of which involve the coordinated nitrogen, that cannot be explained by inductive effects alone.[6] Diadducts of $(R_2PN)_4$ have also been structurally characterized.[6a,7] Monoadducts of S_4N_4, including the protonated derivative,[8] all form a flattened boat structure with loss of the cross-ring S–S interactions.

The crystalline adducts 1,5-$Ph_4P_2N_4S_2H^+BF_4^-$, 1,5-$Ph_4P_2N_4S_2Me^+CF_3SO_3^-$, 1,5-$Ph_4P_2N_4S_2\cdot BCl_3$, and (1,5-$Ph_4P_2N_4S_2)_4\cdot 3SnCl_4$ have been isolated and characterized by ^{31}P NMR, Raman, and, in the case of the $SnCl_4$ adduct, ^{119}Sn Mössbauer spectroscopy. The structure of 1,5-$Ph_4P_2N_4S_2Me^+CF_3SO_3^-$ was determined by X-ray crystallography. The formation of diadducts was monitored by ^{31}P NMR spectroscopy, and the

---

[†] The University of Calgary.

[‡] Concordia University.

(1) Chivers, T.; Liblong, S. W.; Richardson, J. F.; Ziegler, T. *Inorg. Chem.* **1988**, *27*, 4344.

(2) Burford, N.; Chivers, T.; Codding, P. W.; Oakley, R. T. *Inorg. Chem.* **1982**, *21*, 982.

(3) Burford, N.; Chivers, T.; Richardson, J. F. *Inorg. Chem.* **1983**, *22*, 1482.

(4) Burford, N.; Chivers, T.; Rao, M. N. S.; Richardson, J. F. *Inorg. Chem.* **1984**, *24*, 1946.

(5) Chivers, T.; Dhathathreyan, K. S.; Liblong, S. W.; Parks, T. *Inorg. Chem.* **1988**, *27*, 1305.

(6) (a) Trotter, J.; Whitlow, S. H.; Paddock, N. L. *J. Chem. Soc., Chem. Commun.* **1969**, 695. (b) Trotter, J.; Whitlow, S. H. *J. Chem. Soc. A* **1970**, 460.

(7) (a) Calhoun, H. P.; Oakley, R. T.; Paddock, N. L.; Trotter, J. *Can. J. Chem.* **1975**, *53*, 2413. (b) Trotter, J.; Whitlow, S. H. *J. Chem. Soc. A* **1970**, 455.

(8) Cordes, A. W.; Marcellus, C. G.; Noble, M. C.; Oakley, R. T.; Pennington, W. T. *J. Am. Chem. Soc.* **1983**, *105*, 6008.

0020-1669/89/1328-3683$01.50/0

Table I. Raman and ^{31}P NMR Spectroscopic Data for Adducts of **2** (R = Ph)

adduct	ν(S–S),[a] cm^{-1}	$\delta(^{31}P)$[b]	$^4J_{PP}$, Hz
$1,5\text{-}Ph_4P_2N_4S_2H^+BF_4^-$	289	124.6, 95.0	23.1
$1,5\text{-}Ph_4P_2N_4S_2H^+CF_3SO_3^-$[c]		127.3, 88.7	
$1,5\text{-}Ph_4P_2N_4S_2Me^+CF_3SO_3^-$	280	129.3, 83.5	16.1
$1,5\text{-}Ph_4P_2N_4S_2\cdot BCl_3$	288	126.6, 87.6	20.4
$[1,5\text{-}Ph_4P_2N_4S_2H_2^{2+}][CF_3SO_3^-]_2$[d]	*e*	42.3, 35.2 41.8	5.5
$[1,5\text{-}Ph_4P_2N_4S_2Me_2^{2+}][CF_3SO_3^-]_2$[d]	*e*	49.7, 40.8 42.6	3.4
$(1,5\text{-}Ph_4P_2N_4S_2)_4\cdot 3SnCl_4$	282	111.6	
$1,5\text{-}Ph_4P_2N_4S_2$	268	113.9[f]	

[a] Obtained from the Raman spectrum. [b] Chemical shifts relative to 85% H_3PO_4 as external reference. [c] Generated in situ by addition of CH_3CN to a $CDCl_3$ solution of the diprotonated derivative. [d] ^{31}P NMR spectra indicated the formation of both asymmetrically and symmetrically substituted diadducts in solution (see text); only the diprotonated derivative was isolated. [e] Not observed. [f] Data taken from ref 5.

crystalline diprotonated derivative was isolated as a mixture of isomers.

Experimental Section

Reagents and General Procedures. All solvents were dried and distilled before use: methylene dichloride (P_2O_5), hexane, pentane, and diethyl ether (Na), acetonitrile (CaH_2 and P_2O_5). All reactions and the manipulation of moisture-sensitive products were carried out under an atmosphere of nitrogen (99.99% purity) passed through Ridox, P_2O_5, and silica gel. Chemical analyses were performed by the Analytical Services of the Department of Chemistry. The University of Calgary, and by Canadian Microanalytical Service Ltd., Vancouver, BC, Canada.

$1,5\text{-}Ph_4P_2N_4S_2$[5] and $(Ph_PN_3S_2)_nSnCl_4$ (n = 1, 2)[9] were prepared by the literature methods. Other chemicals were obtained from Aldrich Chemical Co. and used as received: BCl_3 (1.0 M solution in hexane), $SnCl_4$ (1.0 M solution in CH_2Cl_2), CF_3SO_3H, CF_3SO_3Me, and $HBF_4\cdot Et_2O$.

Instrumentation. Infrared spectra were recorded as Nujol mulls (KBr windows) or KBr pellets on a Nicolet 5DX FT-IR spectrometer. UV–visible spectra were obtained by using a Cary 219 spectrophotometer. NMR spectra were recorded on a Varian XL-200 instrument. ^1H and ^{13}C chemical shifts are referenced to $CHCl_3$ and are reported in ppm downfield from Me_4Si. ^{31}P chemical shifts are referenced to external 85% H_3PO_4. Raman spectra were obtained on a Jarrel-Ash Model 25-100 double monochromator calibrated with carbon tetrachloride. A Coherent Radiation CR4 argon ion laser fitted with an Innova plasma tube was used to obtain exciting radiation at 514 nm. Spectra were recorded on solid samples in glass capillaries or made up as KBr disks (ca. 10-mm diameter) placed in a glass vial, which was rotated at 1000 rpm to prevent thermal decomposition.

^{119}Sn Mössbauer spectroscopy was performed by using a $Ca^{119m}SnO_3$ 15-mCi γ-ray source purchased from Amersham. The Doppler velocity was obtained by using an Elscint driving system working in the constant-acceleration mode (triangular waveform). The samples, held in a Teflon holder with a tight-fitting cap, were cooled to 15 K by using a Displex helium closed-cycle refrigerator, Model DMX-20, obtained from Air Products. The γ-ray beam transmitted by the thin absorber was measured by a (Tl)NaI scintillation counter obtained from Harshaw and accumulated in a 2K Tracor Northern 7200 multichannel analyzer operating in the multiscaling mode. Spectrum fitting was performed on a CDC Cyber 835 mainframe computer, using GMFP5 software,[10a] which is a modified version of the GMFP program of Ruebenbauer and Birchall.[10b] Isomer shifts were referenced to $CaSnO_3$ at room temperature as zero velocity.

Preparation of $1,5\text{-}Ph_4P_2N_4S_2H^+BF_4^-$. (a) From $HBF_4\cdot Et_2O$. A solution of $HBF_4\cdot Et_2O$ (0.19 g, 1.2 mmol) in 8 mL of CH_2Cl_2 was added dropwise to a stirred solution of $1,5\text{-}Ph_4P_2N_4S_2$ (0.51 g, 1.0 mmol) in 25 mL of CH_2Cl_2, and the mixture was stirred at 23 °C for 16 h. After filtration to remove a small amount of a colorless precipitate, the solvent was removed under vacuum and the pale yellow residue was stirred rapidly with hexane (50 mL) for 6 h. The product was isolated by filtration and identified as $1,5\text{-}Ph_4P_2N_4S_2H^+BF_4^-$ (0.43 g, 0.74 mmol). Anal. Calcd for $C_{24}H_{21}BF_4N_4P_2S_2$: C, 49.84; H, 3.66; N, 9.69. Found: C, 50.85; H, 3.70; N, 9.81. IR (cm^{-1}): 3258 br, w, 3055 m, 1438 vs, 1338 m, 1310 m, 1190 m, 1170 m, 1124 vs, 1103 vs, 1059 vs, 1028 s, 998 s, 911 s, 891 vs, 861 s, 843 vs, 787 m, 739 vs, 732 vs, 701 s, 690 m, 652 m, 564 s, 549 vs, 533 s, 511 s. Raman and ^{31}P NMR spectroscopic data are given in Table I.

Table II. Crystallographic Data for $1,5\text{-}Ph_4P_2N_4S_2Me^+CF_3SO_3^-$

chem formula: $C_{26}H_{23}F_3N_4O_3P_2S_3$	fw: 654.63
a = 14.231 (6) Å	space group: $P2_1/n$ (No. 14)
b = 10.824 (3) Å	T = 23 (1) °C
c = 19.326 (10) Å	λ = 0.71073 Å
β = 100.11 (4)°	ρ_{calcd} = 1.48 g cm^{-3}
V = 2930 (1) $Å^3$	R = 0.075
Z = 4	R_w = 0.078

(b) From $BF_3\cdot OEt_2$. An excess of $BF_3\cdot Et_2O$ (0.29 g, 2.0 mmol) was added by syringe to a stirred solution of $1,5\text{-}Ph_4P_2N_4S_2$ (0.86 g, 1.8 mmol) in 20 mL of CH_2Cl_2, and the mixture was stirred at 23 °C for 1.5 h. The volume of the solution was reduced to 5 mL under vacuum, and the residue was stirred rapidly with hexane (100 mL) at 0 °C for 1 h. The resulting pale yellow solid was isolated by filtration and identified as $1,5\text{-}Ph_4P_2N_4S_2H^+BF_4^-$ (0.85 g, 1.5 mmol) by comparison of IR and ^{31}P NMR spectra with that of an authentic sample.

Preparation of $1,5\text{-}Ph_4P_2N_4S_2Me^+CF_3SO_3^-$. An excess of CF_3SO_3Me (0.15 g, 0.91 mmol) was added by syringe to a stirred solution of $1,5\text{-}Ph_4P_2N_4S_2$ (0.35 g, 0.71 mmol) in 30 mL of CH_2Cl_2, and the mixture was stirred at 23 °C for 2 days. The solvent was removed under vacuum, and the pale yellow solid residue was stirred rapidly with pentane (50 mL) for 16 h. The product was separated by filtration and identified as $1,5\text{-}Ph_4P_2N_4S_2Me^+CF_3SO_3^-$ (0.43 g, 0.66 mmol) by X-ray crystallography. Anal. Calcd for $C_{26}H_{23}F_3N_4O_3P_2S_3$: C, 47.70; H, 3.54; N, 8.56. Found: C, 47.43; H, 3.61; N, 8.25. ^1H NMR (in $CDCl_3$): δ 3.30 (3 H, d, $^3J_{HP}$ = 7.9 Hz). ^{13}C NMR (in $CDCl_3$): δ 35.2 (CH_3, d, $^2J_{CP}$ = 6.5 Hz). IR (cm^{-1}): 2966 m, 1439 m, 1339 w, 1262 vs, 1224 m, 1131 vs, 1103 vs, 1083 vs, 1053 vs, 1030 vs, 997 s, 819 vs, 799 vs, 771 m, 755 m, 742 m, 725 m, 695 s, 636 s, 555 m, 527 s, 516 s. Raman and ^{31}P NMR spectroscopic data are given in Table I.

Preparation of $1,5\text{-}Ph_4P_2N_4S_2\cdot BCl_3$. A solution of BCl_3 (1.0 M in hexane, 1.2 mL) was added by syringe to a stirred solution of $1,5\text{-}Ph_4P_2N_4S_2$ (0.56 g, 1.1 mmol) in 25 mL of CH_2Cl_2, and the mixture was stirred at 23 °C for 1 h. The volume of the solution was reduced to 10 mL under vacuum, and the residue was rapidly stirred with hexane (100 mL) at 0 °C for 1 h. The resulting pale yellow solid was separated by filtration and identified as $1,5\text{-}Ph_4P_2N_4S_2\cdot BCl_3$ (0.68 g, 1.1 mmol). Anal. Calcd for $C_{24}H_{20}BCl_3N_4P_2S_2$: C, 47.44; H, 3.32; N, 9.22. Found: C, 47.48; H, 3.67; N, 9.37. IR (cm^{-1}): 1589 w, 1438 vs, 1135 vs, 1122 s, 1113 vs, 1088 vs, 1027 m, 998 s, 923 s, 854 vs, 841 vs, 791 m, 767 m, 747 s, 736 vs, 726 vs, 688 vs, 658 s, 616 w, 553 vs, 524 vs. Raman and ^{31}P NMR spectroscopic data are given in Table I.

Preparation of $[1,5\text{-}Ph_4P_2N_4S_2H_2^{2+}][CF_3SO_3^-]_2$. A solution of CF_3SO_3H (0.70 g, 4.5 mmol) in 5 mL of CH_2Cl_2 was added dropwise to a stirred solution of $1,5\text{-}Ph_4P_2N_4S_2$ (0.55 g, 1.1 mmol) in 30 mL of CH_2Cl_2, and the mixture was stirred at 23 °C for 2 h. The solvent was removed under vacuum, and the pale yellow residue was stirred rapidly with diethyl ether (60 mL) for 16 h. The product was separated by filtration and identified as $[1,5\text{-}Ph_4P_2N_4S_2H_2^{2+}][CF_3SO_3^-]_2$ (0.82 g, 1.0 mmol). Anal. Calcd for $C_{26}H_{22}F_6N_4O_6P_2S_4$: C, 39.50; H, 2.80; N, 7.09. Found: C, 39.98; H, 3.19; N, 7.32. ^1H NMR (in $CDCl_3$): δ 8.73 (2 H, d, $^2J_{HP}$ = 26 Hz). The ^{31}P NMR spectrum of this product (Table I) indicated that it is a mixture of isomers.

Preparation of $(1,5\text{-}Ph_4P_2N_4S_2)_4\cdot 3SnCl_4$. An excess of $SnCl_4$ (1.0 M in CH_2Cl_2, 1.2 mmol) was added by syringe to a stirred solution of $1,5\text{-}Ph_4P_2N_4S_2$ (0.56 g, 1.1 mmol) in 20 mL of CH_2Cl_2, and the mixture was stirred at 23 °C for 1 day. The volume of the solution was reduced to 5 mL under vacuum, and the residue was stirred with n-pentane (50 mL, 0 °C) for 1 h. The pale yellow precipitate was isolated by filtration and identified as $[1,5\text{-}Ph_4P_2N_4S_2]_4\cdot 3SnCl_4$ (0.67 g, 0.24 mmol). Anal. Calcd for $C_{96}H_{80}Cl_{12}N_{16}P_8S_8Sn_3$: C, 42.03; H, 2.94; Cl, 15.51; N, 8.17; S, 9.31. Calcd for the monoadduct $C_{24}H_{20}N_4P_2S_2SnCl_4$: C, 38.38; H, 2.68; Cl, 18.88, N, 7.46; S, 8.54. Found: C, 42.32; H, 3.15; Cl, 15.34; N, 8.14; S, 9.26. IR (cm^{-1}): 1438 s, 1128 vs, 1095 vs, 1048 vs, 1024 vs, 996 s, 848 m, 765 m, 725 vs, 688 s, 541 vs, 524 vs, 507 m. Raman and ^{31}P NMR spectroscopic data are given in Table I.

X-ray Analysis. Crystals of $1,5\text{-}Ph_4P_2N_4S_2Me^+CF_3SO_3^-$ (**3**) were obtained from a CH_3CN–diethyl ether solution. The crystal data are given in Table II, and experimental details are included as supplementary material. A pale yellow crystal of approximate dimensions 0.5 × 0.5 × 0.6 mm was mounted in a glass capillary under nitrogen in a random

---

(9) Chivers, T.; Liblong, S. W.; Richardson, J. F.; Ziegler, T. *Inorg. Chem.* **1988**, *27*, 860.

(10) (a) Monnier, J.; Dênès, G.; Anderson, R. B. *Can. J. Chem. Eng.* **1984**, *62*, 419. (b) Ruebenbauer, K.; Birchall, T. *Hyperfine Interact.* **1979**, *7*, 125.

orientation. Data were collected on an Enraf-Nonius CAD4 diffractometer. Cell constants on an orientation matrix for data collection were obtained from least-squares refinement, with use of the setting angles of 24 reflections in the range 9° < θ < 15°. The space group was determined by the systematic absences ($h0l$, $h + l = 2n$; $0k0$, $k = 2n$) and from subsequent least-squares refinement. As a check on crystal and electronic stability three representative reflections were measured every 60 min and found to decrease by an average of 8.1%. A linear decay correction was applied. Lorentz and polarization corrections were applied to the data. The data were corrected for absorption by using the program DIFABS.[11] The corrections ranged from 0.77 to 1.45. A secondary extinction correction was applied.[12] The final coefficient, refined in least squares, was 1.1 (3) × 10^{-7} (in absolute units). All computations were performed on a VAX 750 computer using SDP/VAX.[13]

The structure of **3** was solved by using direct methods, which revealed the positions of three S and two P atoms. The remaining atoms were located in succeeding difference Fourier syntheses. All H atoms were included in the refinement but restrained to ride on the atom to which they are bonded. The structure was refined in full-matrix least squares, where the function minimized was $\sum w(|F_o| - |F_c|)^2$. Scattering factors were taken from Cromer and Waber.[14] Anomalous dispersion effects were included in F_c;[14] the values for f' and f'' were those of Cromer.[15] The $CF_3SO_3^-$ anion was found to be highly disordered. The final model for this disorder is best described as two SO_3 groups bonded to a common C atom and sharing a common O atom. The groups of S atoms and unique attached O atoms are in a ratio of 60:40. The CF_3 group is spinning, and the F atoms were modeled by using nine isotropic F atoms with occupancies ranging from 0.1 to 0.7 (see Table III). In the final cycles the positional parameters of all atoms in the $CF_3SO_3^-$ model were held constant, but the thermal parameters for the C and F atoms (isotropic) and the S and O atoms (anisotropic) were refined. In the following discussion it is assumed that the overall effect of the disorder on the cation is minimal. The highest peak in the final difference Fourier had a height of 0.99 e Å^{-1} with an estimated error on σF of 0.07 associated with the $CF_3SO_3^-$ ion. Plots of $\sum w(|F_o| - |F_c|)^2$ versus $|F_o|$, reflection order, $(\sin\theta)/\lambda$, etc. showed no unusual trends. The final atomic coordinated are given in Table III.

Table III. Positional Parameters (×10^4) and B_{eq} Values (×10)[a] for the Non-H Atoms of 1,5-$Ph_4P_2N_4S_2Me^+CF_3SO_3^-$

atom	x	y	z	B, Å^2	occ
S(1)	0.2010 (1)	0.0890 (2)	0.68234 (9)	4.59 (4)	
S(2)	0.0557 (1)	0.0709 (2)	0.59505 (9)	4.82 (4)	
S(3)	0.5168 (2)	0.5710 (4)	0.3017 (2)	7.08 (9)	0.6
S(4)	0.5193 (5)	0.6183 (9)	0.2638 (4)	10.4 (2)	0.4
P(1)	0.2255 (1)	0.0784 (2)	0.54374 (9)	4.87 (4)	
P(2)	0.0800 (2)	0.3082 (2)	0.65566 (9)	4.44 (4)	
F(1)	0.360	0.703	0.260	9.1 (2)*	0.7
F(2)	0.373	0.528	0.299	12.4 (6)*	0.3
F(3)	0.376	0.561	0.189	7.7 (3)*	0.4
F(4)	0.351	0.503	0.237	8.0 (4)*	0.3
F(5)	0.342	0.483	0.269	7.5 (5)*	0.2
F(6)	0.347	0.645	0.291	6.6 (7)*	0.15
F(7)	0.397	0.734	0.230	13 (2)*	0.1
F(8)	0.378	0.517	0.203	9.4 (9)*	0.15
F(9)	0.419	0.630	0.157	8 (1)*	0.1
O(1)	0.559	0.481	0.268	10.0 (2)	1.0
O(2)	0.570	0.693	0.305	15.5 (5)	0.6
O(3)	0.486	0.537	0.363	11.1 (4)	0.6
O(4)	0.515	0.690	0.200	13.1 (6)	0.4
O(5)	0.539	0.665	0.338	13.2 (6)	0.4
N(1)	0.2685 (4)	0.0854 (6)	0.6276 (3)	5.3 (1)	
N(2)	0.1128 (4)	0.0436 (6)	0.5349 (3)	5.7 (1)	
N(3)	0.0269 (4)	0.2108 (5)	0.6007 (3)	5.5 (1)	
N(4)	0.1731 (4)	0.2343 (5)	0.7018 (3)	4.4 (1)	
C(1)	0.2200 (5)	0.2761 (8)	0.7726 (4)	6.7 (2)	
C(2)	0.406	0.591	0.245	10.4 (4)*	1.0
C(11)	0.2864 (5)	−0.0432 (7)	0.5066 (3)	5.0 (2)	
C(12)	0.2487 (6)	−0.0893 (8)	0.4471 (4)	6.4 (2)	
C(13)	0.2987 (6)	−0.1845 (8)	0.4145 (4)	7.6 (2)	
C(14)	0.3820 (6)	−0.2281 (9)	0.4495 (5)	8.1 (2)	
C(15)	0.4191 (6)	−0.184 (1)	0.5145 (6)	10.3 (3)	
C(16)	0.3715 (6)	−0.0887 (9)	0.5441 (5)	8.6 (2)	
C(21)	0.2452 (5)	0.2162 (8)	0.4971 (4)	5.6 (2)	
C(22)	0.3334 (6)	0.2735 (8)	0.5110 (5)	7.2 (2)	
C(23)	0.3519 (7)	0.373 (1)	0.4719 (5)	8.8 (3)	
C(24)	0.2857 (7)	0.417 (1)	0.4204 (5)	10.0 (3)	
C(25)	0.1972 (8)	0.363 (1)	0.4058 (5)	10.3 (3)	
C(26)	0.1745 (7)	0.2603 (9)	0.4445 (4)	7.8 (2)	
C(31)	0.0037 (5)	0.3593 (7)	0.7141 (4)	5.3 (2)	
C(32)	0.0153 (5)	0.4776 (8)	0.7446 (4)	6.4 (2)	
C(33)	−0.0385 (6)	0.5121 (9)	0.7936 4)	8.0 (2)	
C(34)	−0.1015 (7)	0.427 (1)	0.8142 (5)	10.0 (3)	
C(35)	−0.1154 (7)	0.312 (1)	0.7823 (6)	10.3 (3)	
C(36)	−0.0612 (5)	0.2787 (9)	0.7291 (5)	8.6 (2)	
C(41)	−0.1240 (5)	0.4409 (7)	0.6173 (3)	5.0 (2)	
C(42)	0.0607 (6)	0.5266 (9)	0.5847 (4)	7.6 (2)	
C(43)	0.0940 (7)	0.6315 (9)	0.5514 (5)	8.5 (3)	
C(44)	0.1869 (7)	0.6448 (9)	0.5534 (4)	8.4 (3)	
C(45)	0.2527 (7)	0.5581 (9)	0.5857 (5)	8.8 (3)	
C(46)	0.2195 (5)	0.4550 (7)	0.6163 (4)	5.8 (2)	

[a] Starred values denote atoms refined isotropically. Anisotropically refined atoms are given in the form of the isotropic equivalent displacement parameter defined as $^4/_3[a^2B_{11} + b^2B_{22} + c^2B_{33} + ab(\cos\gamma)B_{12} + ac(\cos\beta)B_{13} + bc(\cos\alpha)B_{23}]$.

Results and Discussion

Preparation and Spectroscopic Characterization of Monoadducts of 1,5-$Ph_4P_2N_4S_2$ (2, R = Ph). The adduct of **2** (R = Ph) with BCl_3 and the protonated or methylated derivatives were obtained in high yields by the addition of an excess of the appropriate reagent to a stirred solution of **2** (R = Ph) in CH_2Cl_2. The monoadducts were isolated as moisture-sensitive, pale yellow solids by precipitation upon the addition of a nonpolar solvent. Only the methylated derivative 1,5-$Ph_4P_2N_4S_2Me^+CF_3SO_3^-$ could be recrystallized without dissociation. The reaction of **2** (R = Ph) with either $HBF_4{\cdot}Et_2O$ or $BF_3{\cdot}Et_2O$ led to the formation of the monoprotonated derivative 1,5-$Ph_4P_2N_4S_2H^+BF_4^-$, as was found for $Ph_2PN_3S_2$.[9]

The ^{31}P NMR spectra for the monoadducts of **2** (R = Ph) show two doublets with chemical shifts in the range 83–95 and 125–129 ppm (Table I) on either side of the singlet observed at 114 ppm for the free ligand.[3] The downfield signal is tentatively assigned to the phosphorus attached to the coordinated nitrogen, since the effect of electron withdrawal by the electrophile is expected to be greatest for that phosphorus atom. It has been suggested that low-field ^{31}P NMR chemical shifts for strained ring compounds may be related to relatively narrow endocyclic bond angles at phosphorus.[17,18] Thus, the unusually low field chemical shifts of 114 and 120 ppm for **2** (R = Ph and Me, respectively)[5] may be due to the narrow angles at P of 110–111°[2,3] imposed by the cross-ring S–S bonds; cf. $\delta(^{31}P)$ +20 ppm for $(Ph_2PN)_4$ with ∠NPN = 120°[25a] and +19 ppm for **1** (R = Ph) with ∠NPN = 118°.[3] The fact that the X-ray structural analysis of 1,5-$Ph_4P_2N_4S_2Me^+CF_3SO_3^-$ (vide infra) shows that the smaller endocyclic angle at phosphorus involves the phosphorus atom coordinated to nitrogen provides some support for the proposed assignment of the ^{31}P NMR signals of the monoadducts.

The pale color of the monoadducts suggests that coordination to nitrogen does not result in the destruction of the cross-ring S–S bond in **2** (R = Ph) since the loss of this interaction would give rise to a π-electron-rich ring, which should exhibit a low-energy electronic transition; cf. 1,3-$Ph_4P_2N_4S_2Me^+$.[1] Support for this conclusion comes from the Raman spectra of these adducts, in which the strongest band at 280–290 cm^{-1} (Table I) is attributed to the S–S interaction; cf. ν(S–S) 268 and 250 cm^{-1} for **2** (R = Ph and Me, respectively).[2,3] Furthermore, the higher frequency of this band in the adducts compared to the band in the free ligand indicates a strengthening of the S–S interaction. These conclusions

---

[11] Walker, N.; Stuart, D. *Acta Crystallogr.* **1983**, *A39*, 159.
[12] Zachariasen, W. H. *Acta Crystallogr.* **1963**, *16*, 1139.
[13] Frenz, B. A. The Enraf-Nonius CAD4 SDP—A Real-Time System for Concurrent X-ray Data Collection and Crystal Struture Determination. In *Computing in Crystallography*; Schenk, H., Olthof-Hazelkamp, R., van Konigsveld, H., Bassi, G. C., Eds.; Delft University Press: Delft, Holland, 1978; pp 64–71.
[14] Cromer, D. T.; Waber, J. T. *International Tables for X-ray Crystallography*; Kynoch Press: Birmingham, England, 1974; Vol. IV, Table 2.2B.
[15] Ibers, J. A.; Hamilton, W. C. *Acta Crystallogr.* **1964**, *17*, 781.
[16] See ref 13, Table 2.3.1.
[17] Allen, D. W.; Tebby, J. C. *J. Chem. Soc. B* **1970**, 1527.
[18] Blackburn, G. M.; Cohen, J. S.; Weatherall, I. *Tetrahedron* **1971**, *27*, 2903.

Table IV. Selected Bond Lengths (Å) and Bond Angles (deg) for 1,5-$Ph_4P_2N_4S_2$ (**2**; R = Ph) and 1,5-$Ph_4P_2N_4S_2Me^+CF_3SO_3^-$ (**3**)[a]

	2 (R = Ph)[b]	**3**		**2** (R = Ph)	**3**
P(1)–N(1)	1.623 (3)	1.630 (5)	P(2)–C(41)	1.796 (3)	1.780 (7)
P(2)–N(3)	1.623 (3)	1.591 (6)	N(1)–S(1)	1.596 (3)	1.549 (6)
P(1)–N(2)	1.620 (3)	1.628 (6)	N(3)–S(2)	1.596 (3)	1.577 (7)
P(2)–N(4)	1.620 (3)	1.666 (5)	N(2)–S(2)	1.584 (2)	1.559 (6)
P(1)–C(11)	1.792 (3)	1.794 (8)	N(4)–S(1)	1.584 (2)	1.682 (6)
P(1)–C(21)	1.796 (3)	1.790 (8)	S(1)–S(2)	2.528 (1)	2.437 (2)
P(2)–C(31)	1.792 (3)	1.786 (8)	N(4)–C(1)		1.484 (8)
N(1)–P(1)–N(2)	110.8 (1)	107.8 (3)	C(11)–P(1)–C(21)	105.7 (1)	106.3 (4)
N(3)–P(2)–N(4)	110.8 (1)	106.2 (3)	C(31)–P(2)–C(41)	105.7 (1)	108.2 (4)
P(1)–N(1)–S(1)	120.7 (2)	120.7 (3)	N(1)–P(1)–C(11)	111.5 (1)	108.0 (3)
P(2)–N(3)–S(2)	120.7 (2)	125.7 (4)	N(1)–P(1)–C(21)	108.6 (1)	113.4 (3)
P(1)–N(2)–S(2)	121.2 (2)	120.8 (4)	N(2)–P(1)–C(11)	112.4 (1)	108.9 (3)
P(2)–N(4)–S(1)	121.2 (2)	121.8 (3)	N(2)–P(1)–C(21)	107.5 (1)	112.3 (3)
N(1)–S(1)–S(2)	92.6[c]	94.5 (2)	N(3)–P(2)–C(31)		111.0 (3)
N(3)–S(2)–S(1)	92.6[c]	94.3 (2)	N(3)–P(2)–C(41)		114.7 (3)
N(2)–S(2)–S(1)	92.6[c]	92.3 (2)	N(4)–P(2)–C(31)		108.9 (3)
N(4)–S(1)–S(2)	92.6[c]	91.4 (2)	N(4)–P(2)–C(41)		107.8 (3)
N(1)–S(1)–N(4)	116.1 (1)	112.0 (3)	S(1)–N(4)–C(1)		113.9 (4)
N(2)–S(2)–N(3)	116.1 (1)	114.2 (4)	P(2)–N(4)–C(1)		122.3 (5)

[a] The atomic numbering scheme for **3** is given in Figure 1. [b] Data taken from ref 3. Symmetry-equivalent atoms are as follows: P(1), P(2); N(1), N(3); N(2), N(4); S(1), S(2); C(11), C(31); C(21), C(41). [c] Calculated value from data given in ref 3.

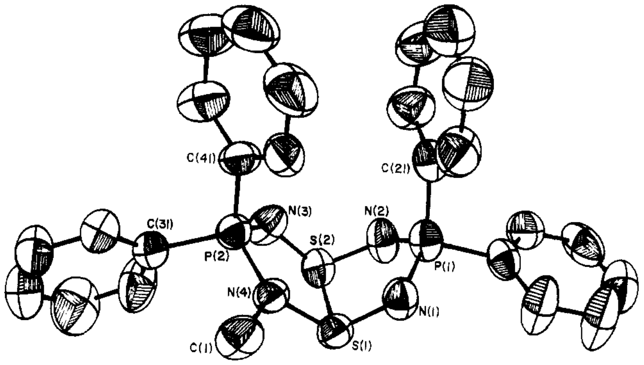

Figure 1. ORTEP plot (50% probability ellipsoids) and atomic numbering scheme for 1,5-$Ph_4P_2N_4S_2Me^+CF_3SO_3^-$ (**3**).

were confirmed by the X-ray structural analysis of 1,5-$Ph_4P_2N_4S_2Me^+CF_3SO_3^-$ described below.

X-ray Crystal Structure of 1,5-$Ph_4P_2N_4S_2Me^+CF_3SO_3^-$ (3). The crystal structure of **3** consists of noninteracting 1,5-$Ph_4P_2N_4S_2Me^+$ and $CF_3SO_3^-$ ions. An ORTEP drawing of the cation of **3** with the atomic numbering scheme is shown in Figure 1. The pertinent bond lengths and bond angles are given in Table IV. As indicated by the spectroscopic results, coordination of a methyl cation to one of the endocyclic nitrogens results in a strengthening of the cross-ring S–S interaction; the S–S distance is 2.437 (2) Å in **3** compared to 2.528 (1) Å in the free ligand.[3] For comparison, MNDO MO calculations for $S_4N_4H^+$ predict a *net strengthening* of the S–S bonds compared to those in S_4N_4, but the cage structure of $S_4N_4H^+$ is unstable with respect to a planar conformation.[8] The folded bicyclic systems can be regarded as two five-membered rings sharing a common S–S bond. However, the planarity of the S_2N_2 units in **3** is somewhat reduced in **3** compared to that in **2** (R = Ph), the N(1)–S(1)–S(2)–N(2) and N(3)–S(2)–S(1)–N(4) moieties being planar to within 0.061 and 0.050 Å, respectively (cf. 0.013 Å for the corresponding planes in **2** (R = Ph)).[3] The angle of intersection between these two planes is also significantly reduced from 117.3° in **2** (R = Ph) to 113.5° in **3**. Furthermore, while the phosphorus atoms lie 0.214 Å below the S_2N_2 planes in **2** (R = Ph),[3] the phosphorus atoms P(1) and P(2) (adjacent to the coordinated nitrogen) in **3** lie out of the S_2N_2 planes by +0.258 and +0.023 Å, respectively. The methyl group is displaced from the opposite side of the plane from P(2) by −0.548 Å.

The P–N and S–N bonds associated with the coordinated nitrogen are, as expected, longer in **3** compared to the corresponding bonds in **2** (R = Ph); this effect is more pronounced for S(1)–N(4) (1.682 vs 1.584 Å) than for N(4)–P(2) (1.666 vs 1.620 Å). The magnitude of these elongations is similar to those observed for the related bonds in $Ph_2PN_3S_2Me^+CF_3SO_3^-$[9] and 1,3-$Ph_4P_2N_4S_2Me^+CF_3SO_3^-$.[1] The other S–N bonds in **3** all show a contraction compared to those in **2** (R = Ph), the effect being greatest for S(1)–N(1) one bond away from the site of methylation. The P–N bonds in the noncoordinated half of the bicyclic system are unaffected by methylation of the adjoining PN_2S_2 ring, while P(2)–N(3), which is one bond removed from the site of methylation, is shortened by ca. 0.03 Å. These changes in bond lengths are discussed in terms of the perturbation of the electronic structure of **2** (R = Ph) by coordination to a CH_3^+ group in the next section.

The enhancement of the S–S cross-ring interaction upon methylation results in a diminution of the endocyclic bond angles at phosphorus from 110.8° in **2** (R = Ph) to 107.8 and 106.2° for P(1) and P(2), respectively, in **3**. The geometry at the coordinated nitrogen atom is essentially planar ($\sum \angle N(4) = 358°$).

Electronic Structure and Bonding in the Methylated Ring 3. A planar $P^V_2N_4S_2$ ring system possesses 10 π electrons. In the limiting case of a folded structure with a transannular S–S σ bond, this number is reduced to eight distributed equally between the two NPN units.[3] However, the S–S distances of ca. 2.5 Å in **2** (R = Me, Ph)[2,3] are substantially longer than the typical S–S single-bond value of 2.05 Å. Thus, it is reasonable to assume that these sulfur atoms participate, to a limited extent, in the π system of this heterocycle. Previous investigations of the effect of adduct formation on the electronic structures of π-electron-rich PNS[1,9] or SN rings[8,19] have shown that many of the observed structural changes, which occur upon coordination of the electrophile, can be rationalized by considering the effects of this perturbation on the π system of the ring. Specifically, the π^*-electron density is polarized toward the coordinated nitrogen in response to the withdrawal of σ-electron density at that nitrogen by the electrophile. In **2** (R = H) the σ and π MOs are not as readily differentiated as they are in $H_2PN_3S_2$. Consequently, we have simplified our model for **2** to a consideration of the perturbation induced by an electrophile on the individual PN_2S_2 units that share a common S–S bond. The composition of the four lowest energy π MOs of the PN_2S_2 ring is illustrated in Figure 2.[20] In the limiting case (vide supra) only $1b_1$ and $1a_2$ would be occupied, but the presence of the S–S interaction suggests a partial contribution from $2b_1$. The bonding characteristics of the π orbitals indicate that polarization of π-electron density toward one of the nitrogens, as a result of coordination to an electrophile, should

---

(19) Marcellus, C. G.; Oakley, R. T.; Cordes, A. W.; Pennington, W. T. *Can. J. Chem.* **1984**, *62*, 1822.

(20) (a) Treu, O., Jr. M.Sc. Thesis, University of São Paulo, São Paulo, Brazil. (b) Treu, O., Jr.; Trsic, M. *J. Mol. Struct.* **1985**, *133*, 1.

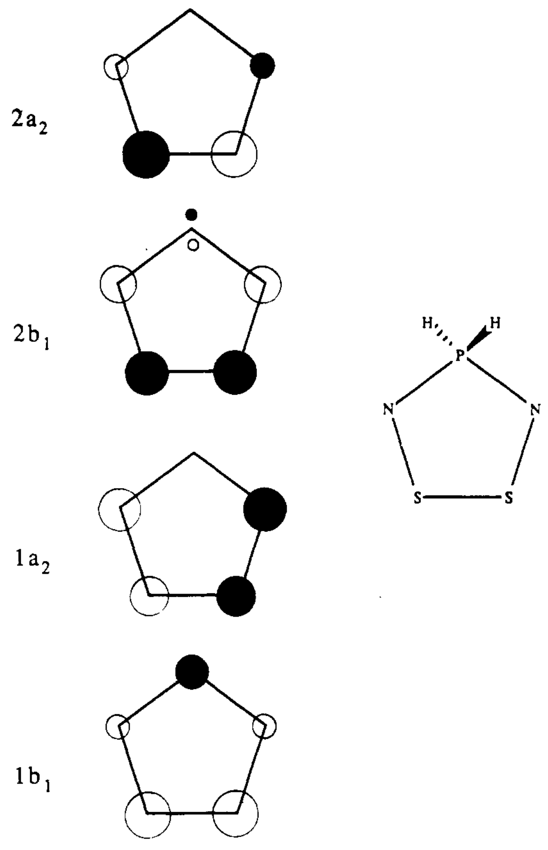

Figure 2. Composition and relative energies of the π molecular orbitals of $H_2PN_2S_2$.

result in a strengthening of the S–S bond, by reduction of the antibonding contribution of $1a_2$ to the net S–S bond order, and weakening of the P–N and S–N bonds associated with the coordinated nitrogen. As a second-order effect the limited contribution of $2b_1$ would be largely offset by the polarization of π-electron density toward the coordinated nitrogen leading to a slight strengthening of the two S–N bonds. The structure of **3** confirms the prediction of a weakening of the bonds involving the coordinated nitrogen and a strengthening of the remaining bonds, especially the S–S interaction, of this PN_2S_2 unit.

The net effect of coordination of a nitrogen to an electrophile on the adjoining PN_2S_2 ring is expected to be only a small reduction in electron density, since delocalization between the two rings is limited. If this effect is restricted to a reduction of the contribution of $2b_1$, one would predict a strengthening of the two S–N bonds ($2b_1$ is antibonding with respect to these bonds) and very little effect on the remote P–N bonds. This prediction is consistent with the observed structure of **3**.

Preparation and Mössbauer Spectra of $(1,5\text{-}Ph_4P_2N_4S_2)_4\cdot 3SnCl_4$ and Related Adducts. The reaction of $1,5\text{-}Ph_4P_2N_4S_2$ with an excess of $SnCl_4$ in methylene dichloride produces an adduct for which elemental analyses (C, H, N, S, and Cl) were in excellent agreement with a 4:3 rather than a 1:1 (or 2:1) stoichiometry. The related complexes *trans*-$(Ph_2PN_3S_2)_2SnCl_4$[9] and *trans*-$(S_4N_4)_2SnCl_4$[21] have been structurally characterized by X-ray crystallography. The ^{119}Sn Mössbauer (MB) data for these adducts are compared in Table V. The IS value for *trans*-L_2SnCl_4 (L = $Ph_2PN_3S_2$, S_4N_4) are in the range found for hexacoordinte tin(IV), and the lack of resolvable quadrupole splitting is not unusual for complexes of this type.[23] A single line (IS = 0.73 mm s^{-1}) is also observed for $(1,5\text{-}Ph_4P_2N_4S_2)_4\cdot 3SnCl_4$, and the line width ($\Gamma$ = 1.57 (3) mm s^{-1}) is indicative of the presence of a small, unresolved quadrupole splitting. This observation is inconsistent with an ionic formulation $[L_2SnCl_3^+]_2[SnCl_6^{2-}]$ for the 4:3 adduct. The resemblance of the MB spectrum of the 4:3 adduct to those of the *trans*-L_2SnCl_4 complexes suggests a structure in which all three tin atoms are in similar *trans*-L_2SnCl_4 environments (Figure 3). This structure should give rise to a singlet for the dicoordinated ligands and a pair of doublets for the monocoordinated ligands in the ^{31}P NMR spectrum. However, the ^{31}P NMR spectrum of the 4:3 adduct in CH_2Cl_2 at 25 °C exhibits a singlet at +111.6 ppm, suggesting an exchange process that results in equivalent phosphorus atoms in the ligand occurs in solution. The diadduct *trans*-$(Ph_2PN_3S_2)_2SnCl_4$ dissociates readily into the monoadduct in solution.[9] A similar dissociative process may occur for $(1,5\text{-}Ph_4P_2N_4S_2)_4\cdot 3SnCl_4$.[24] However, dissociation alone cannot account for the simple ^{31}P NMR spectrum. Site exchange must also be invoked to account for the apparent equivalence of the phosphorus atoms in monocoordinated ligands. Attempts to carry out a variable-temperature ^{31}P NMR study of the 4:3 adduct were thwarted by the insolubility of this complex.

Table V. ^{119}Sn Mössbauer Data for $SnCl_4$ Adducts

adduct	Mössbauer data, mm s^{-1} [a] IS	QS	Γ
$(1,5\text{-}Ph_4P_2N_4S_2)_4\cdot 3SnCl_4$	0.73 (2)	0	1.57 (3)
trans-$(Ph_2PN_3S_2)_2SnCl_4$	0.46 (3)	0	1.42 (3)
trans-$(S_4N_4)_2SnCl_4$[b]	0.45	0	1.39 (6)
$[(Ph_2PN_3S_2)SnCl_4]_n$	0.57 (4)	0	1.57 (5)

[a] At 15 K; error bars are given in parentheses. [b] Data taken from ref 22.

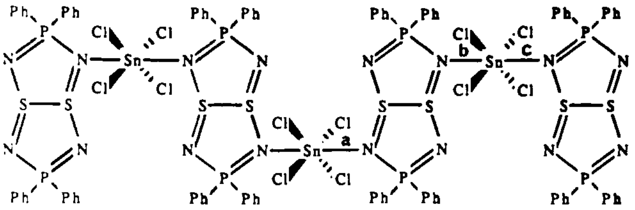

Figure 3. Proposed structure of $(1,5\text{-}Ph_4P_2N_4S_2)_4\cdot 3SnCl_4$.

The monoadduct $[(Ph_2PN_3S_2)SnCl_4]_n$ exhibits a singlet in the MB spectrum (Table V). This observation rules out a trigonal bipyramidal structure for this complex. A polymeric structure in which the tin atoms are in equivalent *trans*-L_2SnCl_4 environments is consistent with the MB data.

Preparation and Spectroscopic Characterization of $[1,5\text{-}Ph_4P_2N_4S_2H_2^{2+}][CF_3SO_3^-]_2$. In contrast to the reaction with HBF_4, the diprotonated adduct $[1,5\text{-}Ph_4P_2N_4S_2H_2^{2+}][CF_3SO_3^-]_2$ rather than the monoprotonated derivative was isolated from the reaction of **2** (R = Ph) with CF_3SO_3H. The ^{31}P NMR spectra data given in Table I indicate that this adduct is a mixture of the isomers **4** and **5** and **6**.

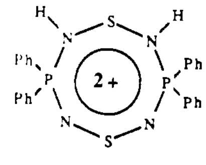

4

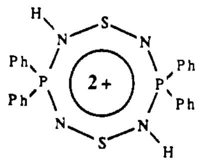

5

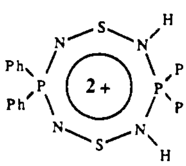

6

The singlet at 41.8 ppm is assigned to one of the symmetrically substituted isomers **4** and **5**. Distal disubstitution to give **5** is more likely on the basis of electrostatic repulsion considerations and previous results for the quaternization of cyclotetraphosphazenes.[7a,25b] The pair of doublets at 35.2 and 42.3 ppm is assigned to the asymmetrically substituted isomer **6**. The

---

(21) Martan, H.; Weiss, J. *Z. Anorg. Allg. Chem.* **1984**, *514*, 107.

(22) Das, M. K.; Bibber, J. W.; Zuckerman, J. J. *Inorg. Chem.* **1982**, *21*, 2864.

(23) Zuckerman, J. J. *Adv. Organomet. Chem.* **1970**, *9*, 21.

(24) Various modes of dissociation can be envisaged involving the rupture of the Sn–N bonds a, b, and c (Figure 3).

(25) (a) Krishnamurthy, S. S.; Sau, A. C.; Woods, M. *Adv. Inorg. Chem. Radiochem.* **1978**, *21*, 92. (b) Allcock, H. R.; Levin, M. L.; Austin, P. E. *Inorg. Chem.* **1986**, *25*, 2281.

pronounced upfield shift for these signals and the smaller coupling constant observed for **6** compared to the corresponding data for the monoadducts suggest that the transannular S–S bond is broken upon coordination of the second proton. The dimethylated derivative $[1,5\text{-}Ph_4P_2N_4S_2Me_2^{2+}][CF_3SO_3^-]_2$ was also generated in solution by treatment of **2** (R = Ph) with an excess of CF_3SO_3Me, and the ^{31}P NMR spectrum indicated a similar mixture of isomers (Table I). The interconversion of these isomers in solution was monitored by ^{31}P NMR spectroscopy. It was observed for the diprotonated derivative that **6** converts into **5** whereas the reverse process occurs for the dimethylated adduct.

The lack of regiospecificity found for the formation of diadducts by **2** (R = Ph) is in contrast to the behavior observed for **1** (R = Ph). Ab initio Hartree–Fock–Slater SCF calculations of the interaction of the model system **2** (R = H), from the experimental geometry for **2** (R = Ph),[3] with two protons to give either **5** or **6** reveal very little difference in the total interaction energy for these two systems.[26] The values are −104 and −108 kcal mol^{-1} for **5** and **6**, respectively, with the difference being primarily due to a slightly larger electrostatic contribution to the interaction energy for **6**. In light of these calculations the lack of regiospecificity in the formation of diadducts of **2** and their tendency to interconvert are not surprising.

Conclusion. The folded structure of **2** (R = Ph) is maintained in monoadducts with Lewis or Brønsted acids, and the transannular S–S interaction is strengthened. A similar enhancement of the S–S bond was predicted for the protonation of S_4N_4,[8] but the cage structure of $S_4N_4H^+$ is unstable with respect to a planar form. This major structural change has been attributed to the polarization of the π^*-electron density of the π-electron-rich ring into the skeletal bonds to the protonated nitrogens. The limited conformational change observed for **2** (R = Ph) upon adduct formation is reminiscent of the behavior of the π-electron-precise cyclotetraphosphazenes. In the limiting case of a full cross-ring S–S bond, **2** (R = Ph) can be viewed as a π-electron-precise system and in practice the π^*-electron density is much lower than that in binary S–N rings. Consequently, the polarization of the π system induced by coordination to an electrophile has a smaller disruptive influence on the skeletal bonds. The nonregiospecific formation of adducts with stoichiometries other than 1:1 is an interesting feature of the Lewis base behavior of **2** that deserves further investigation.

Acknowledgment. We thank the NSERC (Canada) for financial support and a postgraduate scholarship to S.W.L. G.Y.D. thanks the NSERC for a University Research Fellowship and Concordia University and the Programme d'Actions Structurantes of Quebec for financial assistance.

Supplementary Material Available: Tables listing crystallographic and thermal parameters, positional and isotropic thermal parameters for H atoms, all bond lengths and bond angles for non-H atoms, and least-squares planes (9 pages); a table of calculated and observed structure factors (10 pages). Ordering information is given on any current masthead page.

---

[26] For a description of the theoretical method and a definition of the components of the interaction energy, see ref 9.

Contribution from the Carl S. Marvel Laboratories of Chemistry,
Department of Chemistry, University of Arizona, Tucson, Arizona 85721

Monomeric Rhenium(IV) Phenoxides and Their Development from Mononuclear Rhenium Halides with Oxygen and Sulfur Donor Ligands

Ian M. Gardiner, Michael A. Bruck, Pamela A. Wexler, and David E. Wigley*

Received April 11, 1989

The homoleptic phenoxide complexes $Re(DIPP)_4$ (**1**, DIPP = 2,6-diisopropylphenoxide) and $Re(DMP)_4$ (**2**, DMP = 2,6-dimethylphenoxide) have been prepared by the reaction of $ReCl_4(THF)_2$ with $Li(DIPP)\cdot OEt_2$ and $Li(DMP)\cdot THF$, respectively. $Re(DIPP)_4$ crystallizes in the monoclinic space group $P2_1/c$ with $a = 22.657$ (3) Å, $b = 11.498$ (2) Å, $c = 18.605$ (3) Å, $\beta = 110.62$ (1)°, $V = 4536.2$ Å^3, and $Z = 4$ with final $R = 0.035$ and $R_w = 0.044$. While $Re(DIPP)_4$ does not react with the internal acetylenes $RC{\equiv}CR$ (R = Me, Et, Ph), less crowded $Re(DMP)_4$ reacts with $RC{\equiv}CR$ to form the adducts $Re(RC{\equiv}CR)(DMP)_4$ (**3**, R = Me; **4**, R = Et; **5**, R = Ph). The new monomeric halides *trans*-$ReBr_4(THT)_2$ (**6**) and *trans*-$ReCl_4(THT)_2$ (**7**, THT = tetrahydrothiophene) have been prepared in high yield by refluxing K_2ReX_6 in concentrated HX (X = Br, Cl) and THT. Reducing $ReX_4(THT)_2$ with zinc in neat THT yields compounds of the formula *mer*-$ReX_3(THT)_3$ (**8**, X = Br; **9**, X = Cl). *mer*-$ReBr_3(THT)_3$ crystallizes in the orthorhombic space group *Pbca* with $a = 15.300$ (2) Å, $b = 14.976$ (2) Å, $c = 16.969$ (2) Å, $V = 3888.3$ Å^3, and $Z = 8$ with final $R = 0.046$ and $R_w = 0.051$. Cyclic voltammetry studies on compounds **1**–**9** reveal that the Re(III)–Re(IV) couple is accessible for all compounds, and it is seen to shift to more negative potentials as THT is replaced by halide followed by phenoxide.

Introduction

Next to those of molybdenum and tungsten, rhenium catalysts are probably the most widely used for olefin metathesis[1] and remain the catalysts of choice for metathesizing certain functionalized olefins.[2] Compared to that of the group 6 metals, however, the synthetic and mechanistic rhenium chemistry related to metathesis is considerably less developed. Two important principles have emerged from the well-studied group 5[3] and 6[4,5] homogeneous olefin and acetylene metathesis systems: (i) the d^0 configuration seems to be the only relevant oxidation state in either

---

(1) (a) Drăgutan, V.; Balaban, A. T.; Dimonie, M. *Olefin Metathesis and Ring-Opening Polymerization of Cyclo-Olefins*, 2nd revised ed.; Wiley-Interscience: Chichester, England, 1985. (b) Ivin, K. J. *Olefin Metathesis*; Academic Press: London, 1983. (c) Grubbs, R. H. In *Comprehensive Organometallic Chemistry*; Wilkinson, G., Stone, F. G. A., Abel, E. W., Eds.; Pergamon Press: Oxford, England, 1982; Vol. 8, pp 499–551.

(2) (a) Mol, J. C.; Woerlee, E. F. G. *J. Chem. Soc., Chem. Commun.* **1979**, 330. (b) Mol, J. C. *J. Mol. Catal.* **1982**, *15*, 35. (c) Bosma, R. H. A.; van den Aardweg, G. C. N.; Mol. J. C. *J. Organomet. Chem.* **1983**, *255*, 159. (d) Bosma, R. H. A.; van den Aardweg, G. C. N.; Mol, J. C. *Ibid.* **1985**, *280*, 115.

(3) (a) Wallace, K. C.; Dewan, J. C.; Schrock, R. R. *Organometallics* **1986**, *5*, 2162. (b) Rocklage, S. M.; Fellman, J. D.; Rupprecht, G. A.; Messerle, L. W.; Schrock, R. R. *J. Am. Chem. Soc.* **1981**, *103*, 1440. (c) Schrock, R.; Rocklage, S.; Wengrovius, J.; Rupprecht, G.; Fellmann, J. *J. Mol. Catal.* **1980**, *8*, 73.

(4) For examples of olefin metathesis by Mo and W, see: (a) Murdzek, J. S.; Schrock, R. R. *Organometallics* **1987**, *6*, 1373. (b) Schaverien, C. J.; Dewan, J. C.; Schrock, R. R. *J. Am. Chem. Soc.* **1986**, *108*, 2771. (c) Augero, A.; Kress, J.; Osborn, J. A. *J. Chem. Soc., Chem. Commun.* **1986**, 531. (d) Ehrenfeld, D.; Kress, J.; Moore, B. D.; Osborn, J. A.; Schoettel, G. *Ibid.* **1987**, 129. (e) Schrock, R. R.; DePue, R. T.; Feldman, J.; Schaverien, C. J.; Dewan, J. C.; Liu, A. H. *J. Am. Chem. Soc.* **1988**, *110*, 1423.

(5) For acetylene metathesis by Mo and W, see: (a) Churchill, M. R.; Ziller, J. W.; Freudenberger, J. H.; Schrock, R. R. *Organometallics* **1984**, *3*, 1554. (b) Freudenberger, H. J.; Schrock, R. R.; Churchill, M. R.; Rheingold, A. L.; Ziller, J. W. *Ibid.* **1984**, *3*, 1563.

0020-1669/89/1328-3688$01.50/0